

## Mechanistic Evaluation of Arsenite Oxidation in TiO<sub>2</sub> Assisted Photocatalysis

Tielian Xu,<sup>†</sup> Prashant V. Kamat,<sup>‡</sup> and Kevin E. O'Shea<sup>\*,†</sup>

Department of Chemistry and Biochemistry, Florida International University, Miami, Florida 33199, and Radiation Laboratory and Department of Chemical & Biomolecular Engineering, University of Notre Dame, Notre Dame, Indiana 46556

Received: July 20, 2005; In Final Form: August 9, 2005

We report herein a detailed assessment of the roles of O<sub>2</sub>, H<sub>2</sub>O<sub>2</sub>, •OH, and O<sub>2</sub><sup>•-</sup> in the TiO<sub>2</sub> assisted photocatalytic oxidation (PCO) of arsenite. Although both arsenite, As(III), and arsenate, As(V), adsorb extensively onto the surface of TiO<sub>2</sub>, past studies relied primarily on the analysis of the arsenic species in solution, neglecting those adsorbed onto the surface of TiO<sub>2</sub>. We used extraction and analyses of the arsenic species adsorbed onto the surface of the TiO<sub>2</sub> to illustrate that the oxidation of As(III) to As(V) occurs in an adsorbed state during TiO<sub>2</sub> PCO. The TiO<sub>2</sub> photocatalytic oxidation (PCO) of surface adsorbed As(III) in deoxygenated solutions with electron scavengers, Cu<sup>2+</sup>, and polyoxometalates (POM) yields oxidation rates that are comparable to those observed under oxygen saturation, implying the primary role of oxygen is as a scavenger of the conduction band electron. Pulse radiolysis and competition kinetics were employed to determine a rate constant of  $3.6 \times 10^6 \text{ M}^{-1} \text{ s}^{-1}$  for the reaction of As(III) with O<sub>2</sub><sup>•-</sup>. Transient absorption studies of adsorbed hydroxyl radicals, generated by subjecting colloidal TiO<sub>2</sub> to radiolytic conditions, provide convincing evidence that the adsorbed hydroxyl radical (TiO<sub>2</sub>+•OH) plays the central role in the oxidation with As(III) during TiO<sub>2</sub> assisted photocatalysis. Our results suggest the reaction of superoxide anion radical does not contribute in the conversion of As(III) when compared to the reaction of As(III) with •OH radical during TiO<sub>2</sub> PCO.

### Introduction

Arsenic is one of the most problematic water contaminants in the world, and approximately 100 million people are at health risks worldwide due to drinking arsenic contaminated water. The main source of arsenic is geological, but human activities such as mining and pesticides can also cause arsenic pollution.<sup>1,2</sup> The toxicity of arsenic to human health ranges from skin lesions to cancer of the brain, liver, kidney, and stomach.<sup>3,4</sup> Recently, the European Union and the United States government have lowered the maximum contaminant level for total arsenic to 10 μg/L (10 ppb) in drinking water.<sup>5</sup>

Arsenic exists mainly as the As(III) and As(V) oxyanions, arsenite (H<sub>3</sub>AsO<sub>3</sub>) and arsenate (H<sub>3</sub>AsO<sub>4</sub>). The distribution between As(III) and As(V) and their speciation in water depends on redox potential and pH. Under groundwater conditions, As(III) is the predominate form of arsenic, which is much more toxic and mobile than As(V). As(III) has low affinity with mineral surfaces while As(V) adsorbs easily to solid surfaces.<sup>6,7</sup> The oxidation of As(III) to As(V) is highly desirable for enhancing the immobilization of arsenic and is required for most arsenic removal technologies. The most common method of arsenic removal is coagulation with iron salts and/or alumina, followed by microfiltration.<sup>8,9</sup>

TiO<sub>2</sub> assisted photocatalysis is an advanced oxidation process for the remediation of polluted water and air.<sup>10–12</sup> Although the majority of TiO<sub>2</sub> assisted PCO studies involve organic substrates as model pollutants, photocatalytic oxidation of inorganic species has also been demonstrated.<sup>13,14</sup> Advanced oxidation technolo-

gies (AOTs) including TiO<sub>2</sub> PCO, lead to the formation of a number of reactive species, notably hydroxyl radical, hydrogen peroxide and superoxide radical anion. The considerable promise for pollutant destruction by TiO<sub>2</sub> PCO is mainly ascribed to the strong oxidation potential of the photogenerated valence band (VB) holes in TiO<sub>2</sub> ( $E_{\text{VB}} = +2.7 \text{ V vs NHE at pH 7}$ ), which yield •OH from the oxidation of surface adsorbed H<sub>2</sub>O or OH groups.<sup>15</sup>

TiO<sub>2</sub> photocatalysis has tremendous potential for the treatment of arsenic contaminated water. The conversion of As(III) to As(V) in UV-irradiated TiO<sub>2</sub> suspension has been reported by a number of groups.<sup>16–20</sup> Most of these studies assess the conversion of As(III) during TiO<sub>2</sub> photocatalysis by monitoring the As(III) concentrations in solution (typically a minor fraction of the arsenic species) and do not specifically address the extent and conversion of As(III) and As(V) adsorbed (often > 90%)<sup>21</sup> onto the TiO<sub>2</sub>. While it was reported that O<sub>2</sub><sup>•-</sup> is the main oxidant in the conversion of As(III) to As(V) during TiO<sub>2</sub> PCO,<sup>17,18</sup> radiolysis and sonolysis studies indicate that O<sub>2</sub><sup>•-</sup>/HO<sub>2</sub><sup>•</sup> do not appreciably convert As(III) to As(V).<sup>22,23</sup> A number of reports also suggest hydroxyl radical or valence band hole plays a key role in the TiO<sub>2</sub> PCO of As(III).<sup>16,20</sup> Given the conflict surrounding the role of superoxide anion radical and hydroxyl radicals during advanced oxidative treatment and TiO<sub>2</sub> PCO of As(III), we have conducted detailed mechanistic studies in an attempt to resolve the roles of the different reactive species formed at the surface of TiO<sub>2</sub> during photocatalysis. Radiolysis and competitive kinetic studies were used to access the reaction of O<sub>2</sub><sup>•-</sup> with As(III). Radiolysis of TiO<sub>2</sub> colloids was used to generate adsorbed hydroxyl radicals (trapped holes) which decay as a function of the concentration of As(III). This study indicates

<sup>†</sup> Florida International University.

<sup>‡</sup> University of Notre Dame.

the oxidation of As(III) by hydrogen peroxide and superoxide anion radicals are relatively slow compared to oxidation by adsorbed hydroxyl radicals during TiO<sub>2</sub> PCO.

### Experimental Section

**Materials.** Na<sub>2</sub>HAsO<sub>4</sub>·7H<sub>2</sub>O and As<sub>2</sub>O<sub>3</sub> were purchased from Aldrich and used as the source of arsenate and arsenite, respectively. Then, 668 μM solutions were prepared as stock solutions. NaOH, NaBH<sub>4</sub>, phosphate, KSCN, HClO<sub>4</sub>, Cu(NO<sub>3</sub>)<sub>2</sub> and titanium(IV) isopropoxide were reagent grade and used as received from Fisher. HCl was trace metal grade from Fisher and 1-propanol was HPLC grade from Fisher. Reagent grade SiW<sub>12</sub>O<sub>40</sub><sup>4-</sup> (Aldrich) was used as the polyoxometalate (POM). 1,4-Benzoquinone was purchased from Aldrich and purified by sublimation. Titanium dioxide (Degussa P25, CAS Registry No.: 13463-67-7), with an average surface area of 50 m<sup>2</sup>/g, was used as the photocatalyst. Ultrapure water used for the preparation of all solutions was obtained by filtration (US Filter Company) and distillation of deionized water.

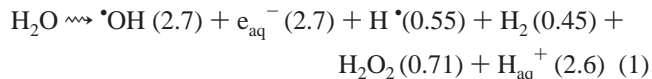
**Photolysis Procedure.** A specific amount of TiO<sub>2</sub> powder was added to arsenite solutions. The TiO<sub>2</sub> aqueous dispersions (100 mL) were mixed on a shaker table in the dark at 300 rpm for 1 h to ensure equilibrium adsorption prior to illumination. The suspensions were transferred to Pyrex reaction vessels (12 × 1 in., 160 mL capacity, Teflon screw top) and purged with air or argon for 15 min and sealed before irradiation. Irradiation of the semiconductor suspensions was conducted in a Rayonet photochemical reactor (Southern New England Ultraviolet), model RPR-100, equipped with 16 phosphor-coated low-pressure mercury lamps (1.5–5 × 10<sup>16</sup> (proton/s)/cm<sup>3</sup>) blazed at 350 nm and a cooling fan.

**Sampling and Extraction.** At given time intervals, 10 mL aliquots were sampled and then centrifuged at 10 000 rpm for 20 min. The supernatant was filtered through a Millipore membrane filter (pore size 0.45 μm) and subsequently analyzed by HPLC-AFS to determine the individual arsenite and arsenate concentrations present in solution. Extraction was required to desorb the arsenic species from the catalyst for analyses. A variety chemical extraction methods have been applied for understanding arsenic bonding and speciation in soils.<sup>7</sup> We tested and modified a number of extraction methods, including ligand exchange, H<sup>+</sup>-enhanced dissolution, and OH<sup>-</sup>-enhanced dissolution in the development of a method to determine the speciation and concentration of arsenic species adsorbed on the surface of TiO<sub>2</sub>. Among the methods tested, extraction with 1 M K<sub>2</sub>HPO<sub>4</sub> was the most effective procedure yielding recoveries of >85% of As(III) and As(V) from the TiO<sub>2</sub> surface. Because of interferences from the high concentration of phosphate, accurate HPLC-AFS detection of arsenite and arsenate individually was not possible, hence a citrate buffer (0.4 M, pH 4.4) was used to selectively measure and monitor As(III).<sup>24</sup> In parallel experiments, the extracts were treated with 12.5% HCl (v/v) and subsequently analyzed by direct AFS for the determination of total arsenic. The As(V) concentration is calculated from the difference in concentrations of total arsenic and As(III).

**Arsenic Analyses.** As(III) and As(V) were determined by a PS Analytical Millennium Excalibur Atomic Fluorescence System, AFS (PSA 10.055) coupled to a HPLC (anion exchange column, PRP X-100, 250 mm × 4.6 mm × 10 μm). Details of the analytical procedures used are described elsewhere.<sup>23</sup>

**Pulse Radiolysis.** Pulse radiolysis experiments were performed utilizing the Notre Dame 8-MeV Titan Beta model TBS-8/16-1S electron linear accelerator with a pulse length of 2.5–10 ns.<sup>25</sup> A typical experiment consisted of a series of 6–10

replicate shots, which were averaged for each determination. For dilute aqueous solutions, the irradiation energy is absorbed mainly by the solvent water, resulting in the formation of a number of reactive species, eq 1.



The *G* values in the parentheses are defined as the number of species formed from 100 eV adsorbed energy. Dosimetry of the system was based on the oxidation of SCN<sup>-</sup> to (SCN)<sub>2</sub><sup>-•</sup> in N<sub>2</sub>O saturated aqueous solutions assuming ε<sub>472 nm</sub>(SCN)<sub>2</sub><sup>-•</sup> = 7580 M<sup>-1</sup> cm<sup>-1</sup> and *G* = 6.13.<sup>26</sup>

**Preparation of Colloids.** In a typical preparation, 2.5 mLs of titanium(IV) isopropoxide was dissolved in 25 mLs of 1-propanol to get 10% titanium(IV) isopropoxide in 1-propanol. A 1 μM TiO<sub>2</sub> colloidal solution was obtained by adding 2.97 μL of 10% titanium(IV) isopropoxide slowly in to 1.0 L of water. The solution pH was adjusted to 1.5 using 1 M HClO<sub>4</sub> to stabilize the TiO<sub>2</sub> colloids.<sup>27</sup>

### Results and Discussion

#### Adsorption and Conversion of As(III) during TiO<sub>2</sub> PCO.

Previous studies on the TiO<sub>2</sub> PCO of arsenite are based primarily on the analyses of the arsenic species in solution, with little or no monitoring of the As(III) and As(V) adsorbed on the surface of TiO<sub>2</sub>. Since the major fraction of arsenic is adsorbed onto TiO<sub>2</sub> surface, we employed an extraction procedure to recover and distinguish the arsenic species bound to the catalyst surface. In a typical experiment, an arsenic containing TiO<sub>2</sub> aqueous suspension was irradiated at 350 nm and samples were taken at specific time intervals. The catalyst was filtered from solution and subjected to an extraction procedure to recover the adsorbed arsenic species. Excellent arsenic mass balances (≥95%) of the surface bound and dissolved arsenic species were obtained throughout our TiO<sub>2</sub> PCO studies. Analyses of the reaction solution and catalyst extracts were conducted to determine the levels of surface bound and dissolved As(III) and As(V).

Dark control experiments confirmed that no appreciable change occurred in the speciation of As(III) and As(V) during extraction or analysis procedures. The adsorption of As(III) onto the surface of the TiO<sub>2</sub> prior to irradiation is greater than 97% under our experimental conditions. The oxidation of As(III) is extremely fast, and within 1 min of irradiation of the TiO<sub>2</sub> suspension >90% of the As(III) has been converted to As(V), as illustrated in Figure 1. Both As(III) and As(V) are strongly adsorbed onto the catalyst with less than 5% in solution. Results from the analyses of the surface bound arsenic fractions confirm the oxidation of As(III) to As(V) occurs at the surface of the catalyst as previously suggested by a kinetic modeling study.<sup>21</sup>

Conversion of As(III) to As(V) by direct photolysis at 350 nm (in the absence of TiO<sub>2</sub>) under air saturated conditions was insignificant (<5%) after 1 h of irradiation and the rates of oxidation in the absence of light or catalyst were also insignificant compared to those observed for TiO<sub>2</sub> PCO. While the control experiments clearly illustrate that the conversion of As(III) involves surface-mediated photocatalysis, the mechanism of the oxidation process is unclear.

The oxidation of As(III) by hydroxyl radical involves the formation of As(IV) which disproportionates to yield As(III) and As(V). As(IV) can also undergo oxidation by dissolved oxygen to form As(V).<sup>28</sup>

TiO<sub>2</sub> PCO involves a complex series of competing reaction processes. Absorption of light greater than the band gap energy

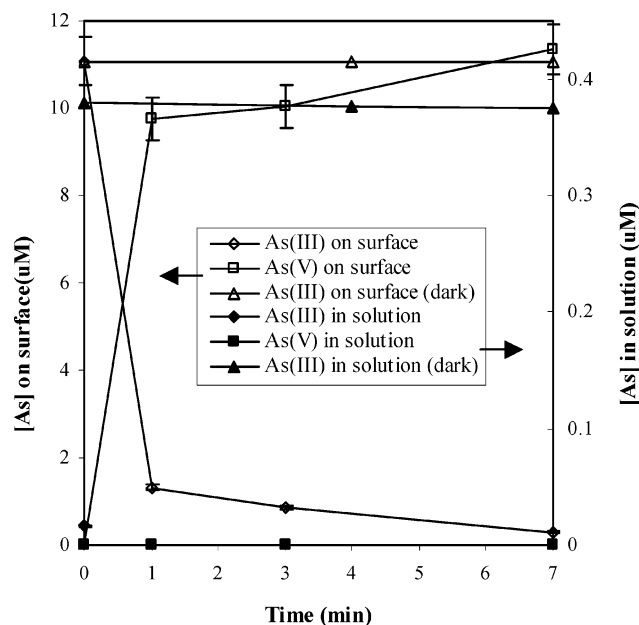
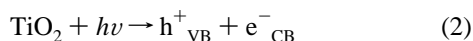
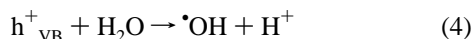


**Figure 1.** Concentration of As(III) and As(V) on the surface of TiO<sub>2</sub> and in solution during TiO<sub>2</sub> PCO. (air saturation, TiO<sub>2</sub> = 1.0 mg/mL, and [As(III)]<sub>0</sub> = 13.4 μM). The experimental error in the analytical measurements is <5% based on triplicate runs.

(wavelengths ≥ 350 nm) results in charge separation producing an electron (e<sup>-</sup><sub>CB</sub>)/hole (h<sup>+</sup><sub>VB</sub>) pair (eq 2).



These charge carriers can recombine, or participate in the redox processes at the interface. Oxygen is commonly used to scavenge the e<sup>-</sup><sub>CB</sub> (eq 3), thus extending the lifetime of the h<sup>+</sup><sub>VB</sub> and promoting oxidation processes at the interface. In aqueous media the h<sup>+</sup><sub>VB</sub> interacts with surface hydroxyl groups and forms surface bound •OH groups, eq 4 and 5.<sup>15</sup> For the purposes of this paper, we will refer the trapped hole and surface adsorbed hydroxyl radical, •OH, as indistinguishable.



While superoxide anion radical and hydrogen peroxide are formed during TiO<sub>2</sub> PCO, •OH is generally believed to play the primary role in promoting oxidation during TiO<sub>2</sub> PCO. The formation of hydrogen peroxide can occur through the combination of two hydroxyl radicals or from reactions of superoxide anion radical. While hydrogen peroxide is formed during TiO<sub>2</sub> PCO given the short reaction time required for conversion of As(III) to As(V), we do not expect an appreciable amount of hydrogen peroxide to be formed. Under our experimental conditions the level of hydrogen peroxide in solution was below the detection limit (20 μM), as determined using the colorimetric method described by Fang et al.<sup>29</sup> At a much higher concentration of H<sub>2</sub>O<sub>2</sub> concentration than expected during the initial stages of TiO<sub>2</sub> PCO, we observe relatively slow conversion of As(III), consistent with the literature.<sup>30</sup> Thus, we conclude the formation of H<sub>2</sub>O<sub>2</sub> and its subsequent reaction leading to the oxidation As(III) were insignificant compared to the conversion of As(III) by TiO<sub>2</sub> PCO.

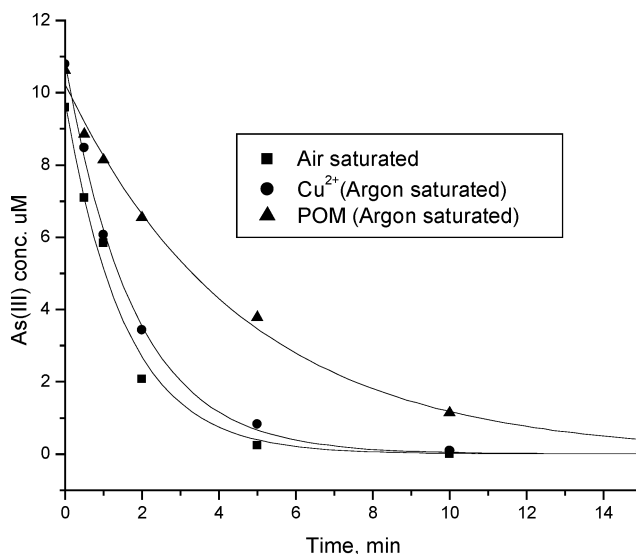


**Figure 2.** Effect of different scavengers on As(III) photocatalysis ([As(III)] = 13.4 μM, TiO<sub>2</sub> = 0.1 mg/mL, [Cu<sup>2+</sup>] and [POM] = 1340 μM).

While hydroxyl radical induced oxidation is generally considered to be the predominant process during TiO<sub>2</sub> PCO, superoxide anion radical can also act as an oxidant. Our results using gamma radiolysis to selectively generate O<sub>2</sub><sup>-•</sup>/HO<sub>2</sub><sup>•</sup> showed minimal conversion of As(III) to As(V).<sup>22</sup> The addition of superoxide dismutase (SOD) to solutions subjected to ultrasonic irradiation (under O<sub>2</sub><sup>-•</sup> or •OH generating conditions) showed no effect on the oxidation of As(III) to As(V), while •OH scavengers had a dramatic effect, indicating •OH-mediated oxidation.<sup>22,23</sup> In contrast recent reports indicate that superoxide anion radical is responsible for the conversion of As(III) during TiO<sub>2</sub> photocatalysis.

To probe the role of oxygen, Cu<sup>2+</sup> and POM (polyoxometalate) were employed as alternate electron scavengers.<sup>31,32</sup> It was reported that the rate of PCO of As(III) is enhanced by POM because POM acts as an electron shuttle between e<sup>-</sup><sub>cb</sub> and O<sub>2</sub>, but the corresponding experiments in the absence of oxygen were not reported.<sup>18</sup> Our control experiments confirm that in the absence of an electron scavenger and in the absence of TiO<sub>2</sub> with any of the employed electron scavengers no conversion of As(III) is observed.

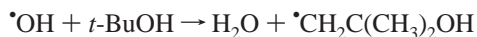
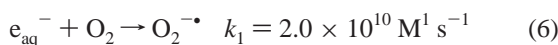
The conversions of As(III) with oxygen as the electron scavenger (air saturated conditions) and under argon saturation with electron scavengers Cu<sup>2+</sup> and POM are illustrated in Figure 2. The concentrations of Cu<sup>2+</sup> and POM were comparable to typical dissolved oxygen concentrations and significantly higher than the concentrations of As(III). With Cu<sup>2+</sup> as the scavenger under argon saturated conditions, the oxidation rate of As(III) is similar to the rate observed under oxygen saturated conditions without Cu<sup>2+</sup>. The rate of As(III) conversion is slightly reduced when POM is the electron scavenger compared to oxygen, possibly the result of back electron transfer and/or relatively weak adsorption of anionic POM at the surface of the catalyst.

These results demonstrate a number of electron scavengers can be used during TiO<sub>2</sub> PCO to effectively oxidize As(III) and the primary role of oxygen appears to be as an electron scavenger. While this does not rule out the possibility that superoxide anion radical can play an important role under oxygenated conditions during PCO, superoxide anion radical is not required for effective oxidation of As(III) during TiO<sub>2</sub> PCO.

### The Reaction of Superoxide Anion Radical with As(III).

Pulse radiolysis techniques have been used to provide tremendous insight into the fundamental mechanistic aspects of TiO<sub>2</sub> PCO. Although pulse radiolysis involves generation of  $\cdot\text{OH}$  and superoxide anion radicals under homogeneous conditions and TiO<sub>2</sub> PCO involves a heterogeneous system, there are strong correlations of the kinetic and mechanistic aspects between the radiolytic and TiO<sub>2</sub> photocatalytic oxidation processes.<sup>33–37</sup>

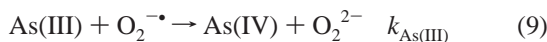
We used pulse radiolysis to study the reactions of superoxide anion radical with As(III) as described below. Under radiolytic conditions, oxygen reacts with hydrated electrons to form superoxide anion radical in a diffusion-controlled reaction, eq 6, with a  $G$  value of 3.2.<sup>38</sup> An excess of *tert*-butyl alcohol 5% (v/v) was added to the solution to scavenge essentially all  $\cdot\text{OH}$  radicals produced during radiolysis, as illustrated by eq 7.<sup>39</sup>



$$k_2 = 6.0 \times 10^8 \text{ M}^{-1} \text{ s}^{-1} \quad (7)$$

Since superoxide anion radical, As(III) and the initial oxidation product, As(IV) possess only weak short wavelength absorptions, we employed 1,4-benzoquinone (BQ) as competitive indicator to determine the rate constant of superoxide anion radical with As(III). The reaction of BQ with  $\text{O}_2^{\cdot-}$  forms a semiquinone radical anion ( $\text{BQ}^{\cdot-}$ ) which can be readily monitored by a characteristic peak at 430 nm using transient absorption spectroscopy.<sup>40</sup>

Using the reaction of BQ with superoxide anion radical as a standard reaction, represented by eq 8, and varying the concentration of As(III) in solution to compete for reaction with superoxide anion radical allows for the determination of the rate constant for eq 9.



On the basis of the competitive reactions of BQ and As(III) with superoxide anion radical the rate constant for the reaction of As(III) with  $\text{O}_2^{\cdot-}$  can be expressed mathematically,<sup>41</sup> by eq 10,

$$\frac{\text{Abs}_{0(\text{BQ}^{\cdot-})}}{\text{Abs}_{(\text{BQ}^{\cdot-})}} = 1 + \frac{k_{\text{As(III)}}[\text{As(III)}]}{k_{\text{BQ}}[\text{BQ}]} \quad (10)$$

where  $\text{Abs}_{0(\text{BQ}^{\cdot-})}$  is the absorbance of the benzoquinone radical anion at 430 nm in the absence of As(III) and  $\text{Abs}_{(\text{BQ}^{\cdot-})}$  is the absorbance at 430 nm in the presence of specific As(III) concentrations. On the basis of this relationship, the rate constant can be determined from the change in absorbance at 430 nm as a function of  $[\text{As(III)}]/[\text{BQ}]$ . The initial As(III) concentration was varied from 0.49 to 10 mM at constant BQ concentration of 0.02 mM to maintain pseudo-first-order conditions. A plot of change in absorbance at 430 nm as a function of  $[\text{As(III)}]/[\text{BQ}]$ , illustrated in Figure 3, yields a linear relationship with slope representing the ratio  $k_{\text{As(III)}}/k_{\text{BQ}}$ . Dividing the slope by the literature value for  $k_{\text{BQ}}$  yields a rate constant of  $3.6 \times 10^6 \text{ M}^{-1} \text{ s}^{-1}$  for the reaction of As(III) with superoxide anion radical.

The rate constant for the reaction of  $\text{HO}^\cdot$  with As(III) is  $8.5 \times 10^9 \text{ M}^{-1} \text{ s}^{-1}$ , more than 3 orders of magnitude faster than  $\text{O}_2^{\cdot-}$  under homogeneous conditions.<sup>28</sup> This observation contradicts Choi et al. remark that superoxide anion radical is

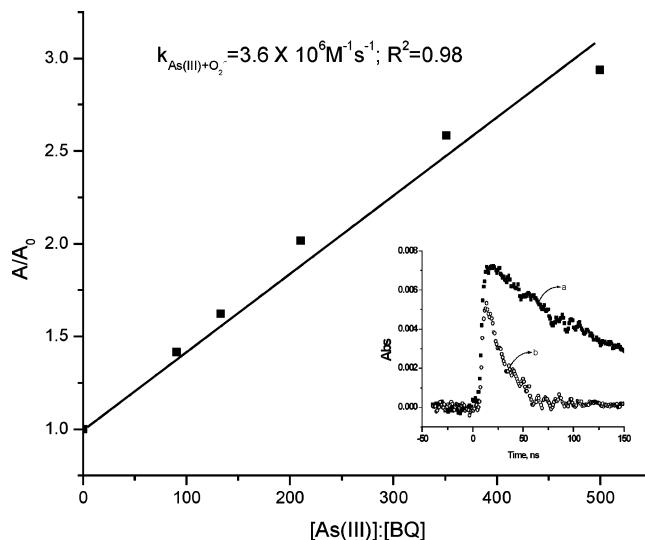
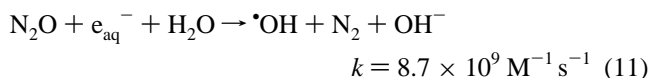


**Figure 3.** Change in absorbance ( $A_0/A$ ) at 430 nm as a function of  $[\text{As(III)}]/[\text{BQ}]$  during pulse radiolysis generation of  $\text{O}_2^{\cdot-}$  ( $\text{O}_2$  saturated; pH 7). The inset shows the growth of the  $\text{BQ}^{\cdot-}$  absorbance at 430 nm (a) without and (b) with 10 mM As(III).

the predominant oxidant during TiO<sub>2</sub> PCO.<sup>17,18</sup> Their conclusion is based in part on differences observed for As(III) oxidation using Pt-modified and naked TiO<sub>2</sub> catalysts. However such a comparison between the two catalyst cannot be taken as evidence since modification with noble metals (Pt, Au, etc.) is expected to increase the efficiency of charge separation and the yield of reductive and oxidative conversions.<sup>42,43</sup> Analogous explanations can be used to rationalize the faster observed rates of As(III) oxidation under humic acid and dye sensitized PCO conditions. Visible light sensitized TiO<sub>2</sub> PCO was employed to produce superoxide anion radical without yielding hydroxyl radicals,<sup>18</sup> however the oxidation of As(III) under such conditions can also occur by type I and II photooxidation processes and thus is also not conclusive to the involvement superoxide anion radical.<sup>44</sup>

Under pulse radiolysis conditions the reaction of As(III) with superoxide anion radical is slow compared to the reaction hydroxyl radical with As(III).

**Reaction of (TiO<sub>2</sub> +  $\cdot\text{OH}$ ) with As(III).** Following the work of Lawless et al, pulse radiolysis and TiO<sub>2</sub> colloids were used to directly monitor the lifetimes of adsorbed hydroxyl radicals at the surface of TiO<sub>2</sub>.<sup>15</sup> Radiolysis of N<sub>2</sub>O-saturated aqueous solutions with high-energy electrons generates primarily  $\cdot\text{OH}$  radicals as N<sub>2</sub>O scavenges hydrated electrons, as shown in Eq 11, to selectively produce hydroxyl radical as the primary radical.<sup>45</sup>



A system consisting of 90%  $\cdot\text{OH}$  radicals was achieved under these conditions with  $G(\cdot\text{OH}) = 5.4$ . Under such conditions in the presence of TiO<sub>2</sub> colloids,  $\cdot\text{OH}$  is trapped at the surface of TiO<sub>2</sub> to form a transient, the same species that is observed during photoexcitation of TiO<sub>2</sub>.<sup>15</sup> The transient is assigned to adsorbed hydroxyl radical/ trapped hole, which will be referred to as (TiO<sub>2</sub> +  $\cdot\text{OH}$ ) for the purposes of this paper. Figure 4 illustrates the absorption spectrum of the transient taken immediately after the pulse to generate (TiO<sub>2</sub> +  $\cdot\text{OH}$ ) in the presence and absence of As(III). The spectrum shows an onset of absorption at wavelengths <470 nm with a maximum at ~360 nm, and is

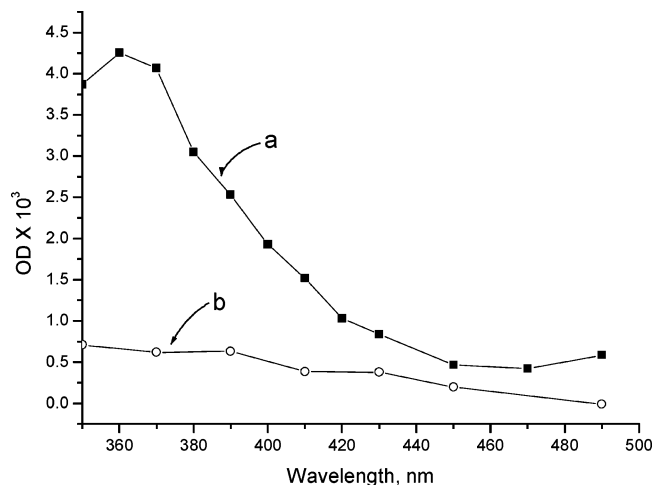
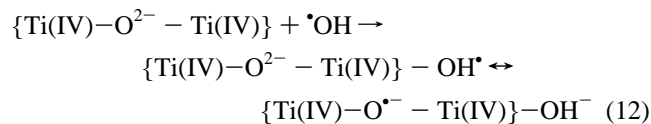
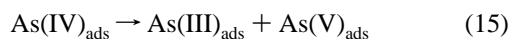
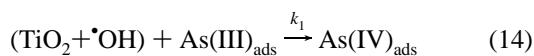
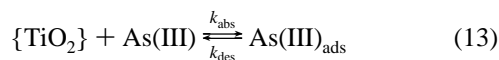


**Figure 4.** Absorbance of  $(\text{TiO}_2 + \bullet\text{OH})$  reaction (a) without As(III) and (b) with 10 mM As(III). ( $\text{TiO}_2$  1.0  $\mu\text{M}$ ; pH 1.5;  $\text{N}_2\text{O}$  saturated; 10 mM As(III)).

attributed to the trapped hole (absorbed hydroxyl radical), eq 12.



The absorbance of As(III, IV, V) does not overlap with the  $(\text{TiO}_2 + \bullet\text{OH})$  absorbance at 370 nm. The rate of decay of the absorption at 370 nm increases with increasing concentration of As(III), as illustrated in Figures 4 and 6. The dependence of the  $(\text{TiO}_2 + \bullet\text{OH})$  decay rate on As(III) concentration is reminiscent of a Langmuir-type adsorption/desorption quasi-equilibrium reported for  $\text{SCN}^-$ .<sup>15</sup> Our proposed mechanism for the oxidation of As(III) is given by the sequence of reactions 13–16.



The rate of decay of the  $(\text{TiO}_2 + \bullet\text{OH})$  transient in the presence of the adsorbed fraction of As(III), may be expressed as

$$\begin{aligned} \text{rate} &= k_{\text{decay}}[(\text{TiO}_2 + \bullet\text{OH})] = \\ &\left( k_1^0 + \frac{k_1 K [\text{As(III)}]}{1 + K [\text{As(III)}]} \right) [(\text{TiO}_2 + \bullet\text{OH})] \quad (17) \end{aligned}$$

where  $k_1^0$  is the intrinsic decay of the  $(\text{TiO}_2 + \bullet\text{OH})$  species,  $2.2 \times 10^5 \text{ s}^{-1}$ , under our experimental conditions and  $k_1$  is the As(III)-dependent first-order decay of  $(\text{TiO}_2 + \bullet\text{OH})$  identified in eq 14. The adsorption–desorption coefficient,  $K$ , is defined by eq 13. The electron-transfer reaction 14 is understood to occur between As(III) and  $(\text{TiO}_2 + \bullet\text{OH})$ , at the surface of the same particle. Figure 6 illustrates the rate of decay as a function of

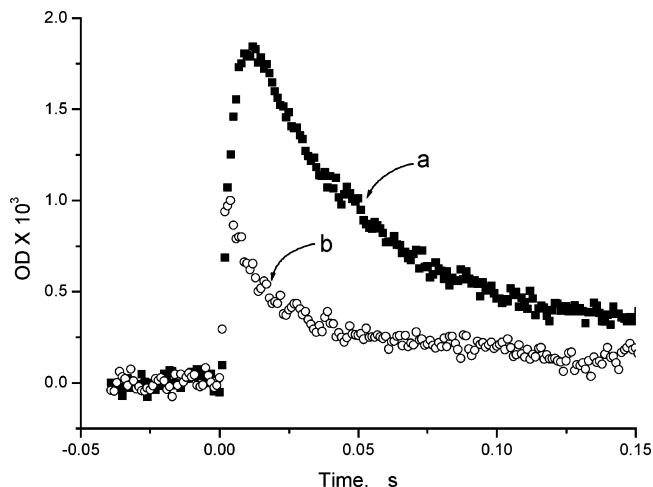


**Figure 5.** Absorption time profile at 370 nm recorded following pulse radiolysis of  $\text{TiO}_2$  colloids (a) in the absence and (b) in the presence of 1.0 mM As(III). ( $\text{TiO}_2$  1.0  $\mu\text{M}$ ; pH 1.5;  $\text{N}_2\text{O}$  saturated).

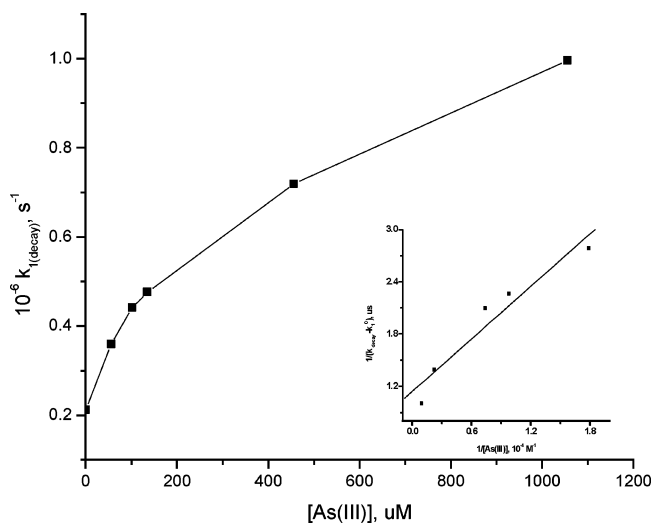


**Figure 6.** Dependence of pseudo-first-order rate constant of  $\text{TiO}_2 + \bullet\text{OH}$  adduct decay at 370 nm as a function of  $[\text{As(III)}]$ . Inset: Langmuir–Hinshelwood analysis of the same result.

$[\text{As(III)}]$  which exhibits a linear dependence as expressed by eq 18.

$$\frac{1}{k_{\text{decay}} - k_1^0} = \frac{1}{k_1} + \frac{1}{k_1 K [\text{As(III)}]} \quad (18)$$

The intercept and slope of the line yield  $k_1 = 8.2 \times 10^5 \text{ s}^{-1}$  and  $K = 3.8 \times 10^3 \text{ M}^{-1}$  ( $r^2 = 0.9926$ ). The value of  $K$  is consistent with previous observation that As(III) strongly adsorbs to the surface of  $\text{TiO}_2$ .<sup>17</sup>

To summarize, our studies indicate that hydroxyl radical plays a key role in the oxidation of As(III) to As(V) during  $\text{TiO}_2$  PCO. It is clear the oxidation of As(III) by  $\text{TiO}_2$  PCO occurs quickly and extensively at the surface of the catalyst. We propose that adsorbed hydroxyl radical oxidizes As(III) to As(IV). The As(VI) can disproportionate at the surface  $\text{TiO}_2$  or be readily oxidized to As(V) by molecular oxygen,  $\bullet\text{OH}$ , etc. Our results indicate that a number of the AOTs, which employ hydroxyl radicals, may be applicable for the oxidation of arsenic in a multistep remediation processes.  $\text{TiO}_2$  PCO can be effectively employed to treat and immobilize arsenic from contaminated drinking water.

**Acknowledgment.** K.E.O. gratefully appreciates the support from the ARCH pilot program (Grant No. S11ES11181) and the Dreyfus foundation. We thank the Radiation Laboratory, University of Notre Dame, for the use of their facilities. P.V.K. acknowledges the support of the Office of the Basic Energy Sciences of the US Department of Energy. This is contribution No. 4624 from the Notre Dame Radiation Laboratory.

## References and Notes

- (1) Jain, C. K.; Ali, I. *Water Res.* **2000**, *34*, 4304–4312.
- (2) Mandal, B. K.; Suzuki, K. T. *Talanta* **2002**, *58*, 201–235.
- (3) Tchounwou, P. B.; Centeno, J. A.; Patlolla, A. K. *Mol. Cell. Biochem.* **2004**, *255*, 47–55.
- (4) Yoshida, T.; Yamauchi, H.; Sun, G. F. *Toxicol. Appl. Pharmacol.* **2004**, *198*, 243–252.
- (5) U.S. EPA *Fed. Regist.* **2001**, *66*, 6976–7066.
- (6) Raven, K. P.; Jain, A.; Loeppert, R. H. *Environ. Sci. Technol.* **1998**, *32*, 344–399.
- (7) Loeppert, R. H.; Jain, A.; El-Haleem, M. A.; Biswas, B. K. Biogeochemistry of Environmentally Important Trace Elements. *ACS Symp. Ser.* **2003**, *835*, 42–56.
- (8) Jekel, M. R. *Arsenic in the Environment, Part I: Cycling and Characterization*; Nriagu, J. O., Eds.; John Wiley & Sons: New York, 1994; pp 119–131.
- (9) Lackovic, J. A.; Nikolaidis, N. P.; Dobbs, G. M. *Environ. Eng. Sci.* **2000**, *17*, 29–39.
- (10) Linsebigler, A. L.; Lu, G.; Yates, J. T. *Chem. Rev.* **1995**, *95*, 735–758.
- (11) Fox, M. A.; Dulay, M. T. *Chem. Rev.* **1993**, *93*, 341–357.
- (12) Hoffmann, M. R.; Martin, S. T.; Choi, W.; Bahnemann, D. W. *Chem. Rev.* **1995**, *95*, 69–96.
- (13) Testa, J. J.; Grela, M. A.; Litter, M. I. *Environ. Sci. Technol.* **2004**, *38*, 1589–1594.
- (14) Prairie, M. R.; Evans, L. R.; Martinez, S. L. *Chem. Oxid.* **1994**, *24*, 2428–2441.
- (15) Lawless, D.; Serpone, N.; Meisel, D. *J. Phys. Chem.* **1991**, *95*, 5166–5170.
- (16) Bissen, M.; Vieillard-Baron, M.; Schindelin, A. *J. Chemosphere* **2001**, *44*, 751–757.
- (17) Lee, H.; Choi, W. *Environ. Sci. Technol.* **2002**, *36*, 3872–3878.
- (18) Ryu, J.; Choi, W. *Environ. Sci. Technol.* **2004**, *38*, 2928–2933.
- (19) Jayaweera, P. M.; Godalumbura, P. I.; Pathiratne, K. A. *Curr. Sci.* **2003**, *84*, 541–534.
- (20) Yang, H.; Lin, W. Y.; Rajeshwar, K. *J. Photochem. Photobiol. A* **1999**, *123*, 137–143.
- (21) Dutta, P. K.; Ray, A. K.; Sharma, V. K.; Millero, F. J. *J. Colloid Interface Sci.* **2004**, *278*, 270–275.
- (22) Xu, T.; Cai, Y.; O'Shea, K. E.; Mezyk, S. In *ACS Symposium Series*; O'Day, P. A., Vlassopoulos, D., Meng, X., Benning, L. G., Eds.; American Chemical Society: Washington DC, 2005; in press.
- (23) Motamedi, S.; Cai, Y.; O'Shea, K. E. In *ACS Symposium Series* 835; Cai, Y.; Braids, O. C., Eds.; American Chemical Society: Washington, DC, 2003; pp 84–94.
- (24) Quinaia, S. P.; Rollemberg, M. C. *J. Braz. Chem. Soc.* **1997**, *8*, 349–356.
- (25) Nicolaescu, A. R.; Wiest, O.; Kamat, P. V. *J. Phys. Chem. A* **2004**, *107*, 427–433.
- (26) Dainton, F. S.; Peterson, D. B. *Proc. R. Soc. London, Ser A* **1962**, *267*, 443–463.
- (27) Bahnemann, D.; Henglein, A.; Lilie, J.; Spanhel, L. *J. Phys. Chem.* **1984**, *88*, 709–711.
- (28) Klaning, U. K.; Bieski, B. H. J.; Sehested, K. *Inorg. Chem.* **1989**, *28*, 2717–2724.
- (29) Fang, X.; Wu, J.; Wei, G.; Schuchmann, H. P.; von Sonntag, C. *Int. J. Radiat. Biol.* **1995**, *68*, 459–466.
- (30) Maurizio, P.; Luigi, C.; Frank, J. M. *Geochim. Cosmochim. Acta* **1999**, *63*, 2727–2735.
- (31) El-Morsi, T. M.; Budakowski, W. R.; Abd-El-Aziz, A. S.; Friesen, K. J. *Environ. Sci. Technol.* **2000**, *34*, 1018–1022.
- (32) Chen, C.; Lei, P.; Ji, H.; Ma, W.; Zhao, J.; Hidaka, H.; Serpone, N. *Environ. Sci. Technol.* **2004**, *38*, 329–337.
- (33) O'Shea, K. E.; Cardona, C. *J. Org. Chem.* **1994**, *59*, 5005–5009.
- (34) O'Shea, K. E.; Kalen, D. V.; Cooper, W. J.; Garcia, I.; Agilar, M. In *Environmental Applications of Ionizing Radiation*, Cooper, W. J., Curry, R., O'Shea, K. E., Eds.; John Wiley and Sons: New York, 1998; p 1569.
- (35) O'Shea, K. E. *Mol. Supramol. Photochem.* **2003**, *10*, 231–247.
- (36) Stafford, U.; Gray, K. A.; Kamat, P. V. *J. Phys. Chem.* **1994**, *98*, 6343–6351.
- (37) Mao, Y.; Schoeneich, C.; Asmus, K. D. *J. Phys. Chem.* **1991**, *95*, 10080–10089.
- (38) Buxton, G. V.; Greenstock, C. L.; Helman, W. P.; Ross, A. B. *J. Phys. Chem. Ref. Data*, **1988**, *17*, 513–886.
- (39) Wolfenden, B. S.; Willson, R. L. *J. Chem. Soc., Perkin Trans.* **1982**, *2*, 805–812.
- (40) Buxton, G. V. In *Pulse Radiolysis*, Tabata, Y., Eds.; CRC Press: Boca Raton, FL, 1991; p 398.
- (41) Spinks, J. W. T.; Woods, R. J. *An Introduction to Radiation Chemistry*, 2nd ed.; John Wiley & Sons: New York, 1976.
- (42) Subramanian, V.; Wolf, E.; Kamat, P. V. *J. Phys. Chem. B* **2001**, *105*, 11439–11446.
- (43) Subramanian, V.; Wolf, E. E.; Kamat, P. V. *J. Am. Chem. Soc.* **2004**, *126*, 4943–4950.
- (44) Foote, C. S. In *ACS Symposium Series 339*; Heitz, J. R., Downum, K. R., Eds.; American Chemical Society: Washington, DC, 1987; pp 22–38.
- (45) Janata, E.; Schuler, R. H. *J. Phys. Chem.* **1982**, *86*, 2078–2084.